New Phytologist

Research

Arabidopsis ubiquitin-specific proteases UBP12 and UBP13 shape ORE1 levels during leaf senescence induced by nitrogen deficiency

Su-Hyun Park[1,2], Jin Seo Jeong[1,2], Jun Sung Seo[2], Bong Soo Park[2] and Nam-Hai Chua[1,2]

[1]Laboratory of Plant Molecular Biology, Rockefeller University, 1230 York Avenue, New York, NY 10065, USA; [2]Temasek Life Sciences Laboratory, 1 Research Link, National University of Singapore, Singapore 117604, Singapore

Author for correspondence:
Nam-Hai Chua
Tel: +65 6872 7001
Email: bchcnh@nus.edu.sg

Received: *4 January 2019*
Accepted: *18 April 2019*

New Phytologist (2019) **223:** 1447–1460
doi: 10.1111/nph.15879

Key words: deubiquitination, leaf senescence, nitrogen deficiency, ORE1, UBP12, UBP13.

Summary

- Nitrogen deficiency (−N) in plants triggers leaf senescence which is regulated by the transcription factor ORE1. Little is known about post-translational regulation of ORE1 in this process. Here, we show that UBP12/UBP13 (ubiquitin-specific protease 12/13) antagonize the action of NLA (nitrogen limitation adaptation) E3 ligase to maintain ORE1 homeostasis.
- *In vitro* pull-down and *in vivo* co-immunoprecipitation assays demonstrated specific binding between UBP12/UBP13 and ORE1. We further analyzed in various genotypes total Chl content and expression levels of senescence-related genes under −N conditions. We found that UBP12/UBP13 can deubiquitinate polyubiquitinated ORE1 *in vitro* and increase the stability of ORE1 *in vivo* in MG132/cycloheximide-chase experiments.
- Plants overexpressing *UBP12/UBP13* display accelerated leaf senescence which is reversed by the *ore1* mutation. By contrast, the senescence phenotype of plants overexpressing *ORE1* is exacerbated by *UBP12/UBP13* overexpression. The expression of senescence-related genes tracks the senescence phenotype. ORE1 protein levels can be elevated by *UBP12/UBP13* overexpression but decreased in *ubp12-2w/13-3*.
- In conclusion, UBP12/UBP13 deubiquitinate ORE1 to stabilize this transcription factor and promote its activity as a positive regulator for leaf senescence under −N conditions. Our study shows that UBP12/UBP13 counteracts the effect of NLA E3 ligase to accelerate leaf senescence under nitrogen starvation.

Introduction

Senescence is a well-orchestrated process and its initiation is dependent on the life cycle of the organism (Lim *et al.*, 2007; Woo *et al.*, 2013). This natural, age-dependent senescence is regulated by several hormones with opposing actions; hormones such as ethylene, jasmonic acid (JA), abscisic acid (ABA) and salicylic acid (SA) promote leaf senescence, whereas cytokinin delays senescence (Jibran *et al.*, 2013; Khan *et al.*, 2014). In addition, leaf senescence can be triggered by nutrient deficiency (Diaz *et al.*, 2008; Masclaux-Daubresse *et al.*, 2010; Have *et al.*, 2017). As a major macronutrient in plants, nitrogen (N) deficiency induces senescence so that the internal stored N resources can be degraded and redistributed to growing parts of the plant (Schulte auf'm Erley *et al.*, 2007; Agüera *et al.*, 2010; Meng *et al.*, 2016).

Studies in the last two decades have shown that leaf senescence involves a multilayered genetic network to reprogram the efficient reutilization of intracellular metabolites and constituents (Woo *et al.*, 2013) and the NAC-domain transcription factor *ORESARA1* (*ORE1*) plays a major role in this process. During leaf senescence *ORE1* transcription is activated by *ETHYLENE INSENSITIVE 2* (*EIN2*); by contrast, similar to the case of *NAC1* (Guo *et al.*, 2005), *ORE1* mRNA is negatively regulated via *miRNA164*-mediated cleavage (Kim *et al.*, 2009). Increased levels of ORE1 protein lead to an increase in transcript levels of downstream senescence-associated genes (SAGs) such as *BFN1*, *RNS3*, *SAG29*, *SINA1* (Matallana-Ramirez *et al.*, 2013) and *NYE1* (Qiu *et al.*, 2015). ORE1 also interferes with chloroplast development and maintenance by binding to the G2-like transcription factors (GLK1 and GLK2), which are critical for chloroplast functions (Rauf *et al.*, 2013). Recently, Kim *et al.* (2018) reported the transcriptional activation of *ORE1* by a core circadian clock complex PSEUDO-RESPONSE REGULATOR9 (PRR9) thereby linking senescence and the clock. Whereas there is information on the transcriptional and post-transcriptional regulation of *ORE1*, little is known regarding possible post-translational regulation of the ORE1 protein.

Because *ORE1* mRNA levels are kept in check by *miR164*, it is reasonable to assume that the ORE1 protein would be unstable, as is the case with *NAC1*/*miR164* (Xie *et al.*, 2002; Guo *et al.*, 2005). Degradation of intracellular proteins in eukaryotes is signaled by ubiquitination, which requires the combined activity of

© 2019 The Authors
New Phytologist © 2019 New Phytologist Trust

a ubiquitin-activating enzyme (E1), a ubiquitin-conjugating enzyme (E2) and a ubiquitin-ligase enzyme (E3). Polyubiquitinated proteins are then sent to 26S proteasomes for degradation. On the other hand, polyubiquitinated proteins can be rescued from destruction by the action of deubiquitination enzymes (DUBs) which remove ubiquitin (Nijman *et al.*, 2005). DUBs are classified into two major types, metalloproteases with JAMM-domain (Verma *et al.*, 2002) and cysteine proteases. The latter can be further categorized into four families according to their functional domains and structures (Wilkinson, 1997; Amerik & Hochstrasser, 2004; Nijman *et al.*, 2005): ubiquitin-specific proteases (UBPs, or USPs in mammals, Hu *et al.*, 2002); ubiquitin C-terminal hydrolases (UCHs, Johnston *et al.*, 1997, 1999); ovarian tumor proteases (OTUs); and Machado–Joseph disease protein domain proteases (MJDs) (Balakirev *et al.*, 2003; Burnett *et al.*, 2003; Scheel *et al.*, 2003; Nanao *et al.*, 2004). UBPs are the largest subfamily of DUBs with diverse functions in yeasts, mammals and plants. Zhou *et al.* (2017) recently reviewed global functions of *Arabidopsis* UBPs involved in various biological processes in plants subject to different environmental stimuli and during growth and development.

Based on their conserved structural domains 27 *Arabidopsis* UBPs have been characterized (Yan *et al.*, 2000; Liu *et al.*, 2008). Among these, UBP12 and UBP13 share high sequence homology (91%) and are known to have redundant functions. Other than their role in plant immunity responses (Ewan *et al.*, 2011), these two UBPs also regulate genes involved in circadian rhythm and flowering time (Cui *et al.*, 2013). The pleiotropic phenotype of *ubp12-2w/13-3* (Cui *et al.*, 2013) suggests that UBP12/UBP13 execute multiple functions during growth and development, most of which remain to be identified. One approach toward elucidating UBP functions and mechanism of action is to identify their direct targets. Recently, UBP12 and UBP13 have been shown to be associated with the plant-specific PcG (polycomb group) protein LIKE HETEROCHROMATIN PROTEIN 1 (LHP1) and to deubiquitinate H2Aub repressing expression of a set of target genes (Derkacheva *et al.*, 2016). In addition, these two UBPs also serve as positive regulators of JA response by deubiquitinating MYC2 (Jeong *et al.*, 2017) and interact with ROOT MERISTEM GROWTH FACTOR 1 (RGF1) to regulate root meristem maintenance (An *et al.*, 2018).

Jeong *et al.* (2017) observed that *ubp12/ubp13 RNAi* lines showed delayed leaf senescence compared to the wild type (WT) upon JA treatment. Here, we found that *ubp12-2w/13-3* plants flower early but display delayed leaf senescence under normal growth conditions as well as under nitrogen deficiency (−N). Consistent with this finding, plants overexpressing UBP12 and UBP13 display accelerated senescence, indicating that this process is promoted by the two UBPs. We identified ORE1, a key transcription factor in leaf senescence, as an interacting protein of UBP12/UBP13 and showed that UBP12/UBP13 can deubiquitinate polyubiquitinated ORE1 *in vitro*. The *in vitro* interaction between UBP12/UBP13 and ORE1 was recapitulated *in vivo*. Analysis of ORE1 protein levels in various genotypic backgrounds provides evidence that UBP12 and UBP13 stabilize ORE1 protein during leaf senescence induced by −N.

Materials and Methods

Plant materials

Arabidopsis thaliana ecotype Col-0 was used as WT. T-DNA insertion mutant lines were used: *ore1* (SALK_090154C), *ubp12-2w* (GABI_742C10), *ubp13-3* (SALK_132368), *ubp12-2w/13-3* (double mutant; Cui *et al.*, 2013) and *nla* (CS858095). Triple mutant *ubp12-2w/13-3/ore1* was obtained by genetic crosses. $ORE1^{OE}$ was a *35S:ORE1-HA*-overexpressing plant in WT. $UBP12^{OE}$ and $UBP13^{OE}$ were WT plants expressing *UBQ10:UBP12-myc* and *UBQ10:UBP13-myc*, respectively. $ORE1^{OE}$/*ubp12-2w*, $ORE1^{OE}$/*ubp13-3*, $ORE1^{OE}$/*ubp12-2w/ubp13-3*, $UBP12^{OE}/ORE1^{OE}$, $UBP12^{OE}$/*ore1*, $UBP13^{OE}/ORE1^{OE}$ and $UBP13^{OE}$/*ore1* were different plants of different genotypes transformed with $ORE1^{OE}$, $UBP12^{OE}$ and $UBP13^{OE}$, respectively. *XVE:UBP12-myc* and *XVE:UBP13-myc* were transgenic plants carrying β-estradiol-inducible (Zuo *et al.*, 2002) UBP12-myc and UBP13-myc, respectively. All transgenic plants were generated by floral dipping with *Agrobacterium* strain GV3101 carrying the relevant constructs (Clough & Bent, 1998; Zhang *et al.*, 2006).

Normal growth and nitrogen deficiency conditions

Seeds were geminated on MS solid medium, pH 5.7, with 0.8% agar. To observe leaf senescence induced by nitrogen deficiency, 3-wk-old seedlings grown on MS solid medium were washed with distilled water several times before being transferred to 1% agar MGRL medium (Fujiwara *et al.*, 1992) and modified MGRL containing 2 mM $CaCl_2$ and 3 mM KCl instead of 2 mM $Ca(NO_3)_2$ and 3 mM KNO_3 and grown under 16 h light (100 μmol m^{-2} s^{-1}) : 8 h dark at 22°C for 2 wk.

Plasmid DNA constructions

ORE1, *NAC1*, *UBP12*, *UBP13*, *UBP14* and *NLA* coding sequences were produced from reverse transcription PCR (RT-PCR). Plasmid DNA for recombinant proteins such as MBP-ORE1-myc, MBP-NAC1-myc, MBP-NLA-myc, GST-UBP12, GST-UBP13 and GST-UBP14 was generated as described by Jeong *et al.* (2017). Constructs for plants carrying *35S:ORE1-HA*, *35S:NAC1-HA*, *35S:UBP14-myc*, *XVE:UBP12-myc*, *XVE:UBP13-myc* and bimolecular fluorescence complementation (BiFC) *35S:nYFP-ORE1* were generated via gateway pENTR/D-TOPO Cloning Kits (Cat no. K240020; Invitrogen) and LR Clonase II Enzyme cloning (Cat no. 11791100; Invitrogen). The constructs *35S:UBP12-cYFP* and *35S:UBP13-cYFP* were described by Jeong *et al.* (2017). The *Arabidopsis UBQ10* (At4g05320) promoter was used to construct *UBQ10:UBP12-myc* and *UBQ10:UBP13-myc*, to avoid possible cosuppression of transgenes transcribed from the *35S*

© 2019 The Authors
New Phytologist © 2019 New Phytologist Trust

promoter. The primers used in this study are listed in Supporting Information Table S1.

Chl content measurement

Leaves were placed in a new tube and weighed. The leaves were homogenized with beads in 80% acetone. Total Chl content (Chl*a* + *b*) was calculated according to Arnon (1949). The Chl content of six biological replicates was measured and the average value presented with standard deviation (±SD). Data derived from different genotypes were compared with WT control by a two-tailed *t*-test statistical analysis (*, $P < 0.05$; **, $P < 0.01$).

Quantitative RT-PCR analysis

Total RNAs were isolated by Trizol (Cat no. 15596026; Invitrogen) or RNeasy mini kit (Cat no. 74104; Qiagen) with DNase I (Cat no. 79254; Qiagen). After synthesis of first-strand cDNA with 1 μg of total RNA (Cat no. 18080-051; Invitrogen), quantitative RT-PCR (qRT-PCR) was performed with the synthesized cDNA and coding sequence-specific primers for *BFN1*, *NYE1*, *SAG29*, *VNI2*, *RNS3*, *ORE1*, *UBP12* and *UBP13* by using SYBR Premix Ex Taq (Cat no. RR420A; Takara, Shiga, Japan) premix and analyzed by using a CFX96 Real-Time PCR system (Bio-Rad). All qRT-PCR experiments were performed with three technical replicates and normalized with *ACT2* transcript levels. The average value of at least three independent biological replicates ($n = 3$) is presented (±SD). The qRT-PCR data were compared with its control by a two-tailed *t*-test (*, $P < 0.05$; **, $P < 0.01$). The primers used in this study are listed in Table S1.

In vitro protein binding assays

Constructs for *MBP-ORE1-myc*, *MBP-NAC1-myc*, *MBP-NLA-myc*, *GST-UBP12*, *GST-UBP13*, *GST-UBP14* and *GST* were transformed into *Escherichia coli* strain BL21 (DE3) pLysS (Cat no. 69451; Novagen, Madison, WI, USA). Recombinant protein purification and *in vitro* protein binding assays were described by Jeong *et al.* (2017). Briefly, recombinant proteins were induced by IPTG (isopropyl-β-D-thiogalactoside) and purified using Amylose resin (Cat no. E8021; New England Biolabs, Ipswich, MA, USA) for the MBP tag or Glutathione Sepharose 4 Fast Flow (Cat no. 17-5132-01; GE Healthcare, Piscataway, NJ, USA) for the GST tag. Purified recombinant proteins were washed and eluted according to the manufacturer's instructions. GST resin-bound proteins GST, GST-UBP12, GST-UBP13 and GST-UBP14 were individually incubated with MBP-ORE1-myc or MBP-NAC1-myc. Pulled-down proteins were separated by 10% SDS-PAGE analysis and immunoblotted on Immobilon-P PVDF (Cat no. IPVH00010; Millipore, Billerica, MA, USA) and bands were detected with anti-myc (Cat no. SC-789, Lot no. E1414; Santa Cruz, Santa Cruz, CA, USA) and ECL Prime Western Blotting System (Cat no. RPN2232; GE Healthcare) following the manufacturer's instructions. In all experiments, 2 μg of recombinant proteins was used as shown in the input panels.

Transient expressions in tobacco

Plasmid DNAs for *35S:ORE1-HA*, *35S:NAC1-HA*, *UBQ10:UBP12-myc*, *UBQ10:UBP13-myc* and *35S:UBP14-myc* were introduced into *Agrobacterium* strain GV3101. Infiltration of the *Agrobacterium* was as described by Park *et al.* (2014). Briefly, grown *Agrobacteria* cells in a suspension containing 10 mM $MgCl_2$ with 200 μM acetosyringone (Cat no. D134406; Sigma Aldrich) and 50 μM MG132 (Cat no. 474790; Calbiochem) were infiltrated into 1-month-old tobacco leaves, and the infiltrated plants were then incubated for 3 d. Co-immunoprecipitation (Co-IP) assays were performed using extracts derived from 0.5 g of ground leaves.

In vivo co-immunoprecipitation assay

Twenty 10-d-old seedlings of *XVE:UBP12-myc/35S:ORE1-HA* and *XVE:UBP13-myc/35S:ORE1-HA* were transferred to MS liquid medium containing 50 μM MG132 (Cat no. 474790; Calbiochem) with/without 25 μM β-estradiol (Cat no. E8875; Sigma) and incubated for 16 h at 22°C under continuous light conditions. Harvested seedlings were disrupted in a tube with Co-IP buffer (Jeong *et al.*, 2017) and total proteins were extracted. An aliquot of the total protein extract was saved as an input sample. As a precleaning step to remove adventitious proteins, protein A-agarose was added to the remaining extract and incubated for 1 h at 4°C by frequent inversions of the reaction tube. After removing protein A-agarose by centrifugation, the supernatants were mixed with antibodies, anti-HA (Cat no. SC-805, Lot no. H1215; Santa Cruz), anti-myc (Cat no. SC-789, Lot no. E1414; Santa Cruz), anti-MBP (Cat no. SC-809, Lot no. D2909; Santa Cruz) or without any antibody (−Ab) for 2 h at 4°C and 20 μl of protein A-agarose were added and incubated for 2 h at 4°C. After washing the protein A-agarose/antibody/proteins complexes with Co-IP buffer three or four times, immunoblotting analyses were performed to detect the immunoprecipitated proteins using anti-HA (Cat no. SC-7392, Lot no. A0418; Santa Cruz) and anti-myc (Cat no. SC-40, Lot no. G0913; Santa Cruz) antibodies.

Bimolecular fluorescence complementation assays

The entry clones 35S:*nYFP-ORE1*, *35S:UBP12-cYFP* and *35S:UBP13-cYFP* and empty vector controls were transformed into competent *Agrobacterium* strain GV3101 using a freeze and thaw method. Cultured cells were harvested and resuspended in 10 mM $MgCl_2$ plus 150 μM acetosyringone (Cat no. D134406; Sigma Aldrich) and then kept at 25°C for 3 h without shaking. *Agrobacterium* suspensions were infiltrated into leaves of *Nicotiana benthamiana* using a 2 ml syringe without needle. Images were observed using an LSM 510 laser scanning confocal microscope (Zeiss) 2 d after infiltration.

© 2019 The Authors
New Phytologist © 2019 New Phytologist Trust

Deubiquitination assay *in vitro*

Polyubiquitinated MBP-ORE1 was obtained by an *in vitro* ubiquitination reaction. In total, 600 ng of MBP-ORE1 was mixed with ubiquitination buffer (50 mM Tris pH 7.4, 5 mM $MgCl_2$, 2 mM dithiothreitol (DTT), 2 mM ATP, 100 μM $ZnCl_2$) and 300 ng UBE1 (E1; BostonBiochem, Cat no. E-300), 300 ng of UbcH6 (E2; BostonBiochem, Cat no. E2-630), 600 ng of GST-NLA (E3) and 4 μg of GST-Ubiquitin (BostonBiochem, Cat no. U-540) in a total volume of 40 μl. After incubation for 4 h at 30°C, the reaction mixture is treated with 20 mM EDTA pH 8.0 to stop the continuous ubiquitination by inhibiting enzyme activity of NLA (nitrogen limitation adaptation), which is a RING domain E3 ligase. The polyubiquitinated protein-containing mixture diluted to 1 : 5 was then used as a substrate for deubiquitination. To this purified protein, 500 ng of GST-UBP12, GST-UBP13 or GST-UBP14 was added within deubiquitination buffer (50 mM Tris-HCl pH 7.4, 150 mM NaCl, 5 mM $MgCl_2$ and 2 mM DTT) and the mixture incubated at 30°C for 1, 2 and 3 h in the short-time course experiment. The incubation time was extended to 4, 6 and 8 h for the long-time course experiment. Deubiquitinated MBP-ORE1 proteins were identified by 8% SDS-PAGE followed by immunoblotting using anti-MBP antibody (Santa Cruz; Cat no. SC-809, Lot no. D2909). Self-ubiquitination of MBP-NLA E3 ligase was carried out in same manner as a negative control.

ORE1 protein stability in plants overexpressing UBP12 and UBP13

Ten-day-old seedlings of $ORE1^{OE}$, $UBP12^{OE}/ORE1^{OE}$, $UBP13^{OE}/ORE1^{OE}$ and $ORE1^{OE}/ubp12\text{-}2w/13\text{-}3$ were transferred to nitrogen-deficient liquid medium and incubated for an additional 4 d. Two different lines of each transgenic genotype were treated with/without 50 μM MG132 for 16 h. To examine the half-life of ORE1-HA proteins of those genotypes, seedlings incubated with 50 μM MG132 for 16 h were washed and transferred to a medium containing 200 μM cycloheximide (Cat no. C1988; Sigma-Aldrich). After treatment, seedling samples were harvested at different times and protein extracts were analyzed by immunoblotting using anti-HA antibody (Cat no. SC-7392, Lot no. A0418; Santa Cruz) for ORE1-HA and anti-myc antibody (Cat no. SC-40, Lot no. G0913; Santa Cruz) for UBP12-myc and UBP13-myc. β-Actin levels were used as a loading control and detected by β-actin antibody (Cat no. SC-47778, Lot no. E2317; Santa Cruz). Western blot band intensity was measured using NIH ImageJ software.

Accession numbers

Genes and their accession numbers used in this study are as follows: *UBP12* (At5g06600), *UBP13* (At3g11910), *ORE1* (At5g39610), *NAC1* (At1g56010), *UBP14* (At3g20630), *NLA* (At1g02860), *BFN1* (At1g11190), *NYE1* (At4g22920), *SAG29* (At5g13170), *VNI2* (At5g13180), *RNS3* (At1g26820) and *ACT2* (At3g18780).

Results

Leaf senescence is delayed in *ubp12-2w/13-3*

WT and *ubp12-2w/13-3* plants were grown on soil until 5 and 6 wk after germination. Leaf senescence of WT became apparent when plants reached 5 wk and rapidly progressed in 6-wk-old plants. By contrast, leaf senescence of *ubp12-2w/13-3* plants was delayed and the leaves stayed green even at 6 wk after germination (Fig. 1a). Transcript levels of senescence-related genes were elevated in leaves of 5- and 6-wk-old WT plants. The values were increased up to 40-fold in *BFN1*, 23-fold in *SAG29*, 30-fold in *NYE1* and 5-fold in *VNI2* in leaves of 6-wk-old plants. By contrast, only *SAG29* and *NYE1* were increased 10- and 4-fold, respectively, in leaves of 6-wk-old *ubp12-2w/13-3* plants (Fig. 1b). Consistent with the senescence phenotype, total Chl content in WT leaves was lower than that in *ubp12-2w/13-3* leaves of 5- and 6-wk-old plants (Fig. 1c). These results suggest

Fig. 1 Leaf senescence phenotype in *Arabidopsis thaliana* wild type (WT, Col-0) and *ubp12-2w/13-3* double mutant under normal and nitrogen-deficient conditions. (a) Comparison of leaves between WT and *ubp12-2w/13-3* under normal growth conditions. Seeds were germinated and grown on MS medium for 10 d. Seedlings were transferred onto soil and grown until 5 and 6 wk after germination under 16 h light (100 μmol m^{-2} s^{-1}) : 8 h dark at 22°C ($n = 3$ independent biological replicates). All rosette leaves including petioles and first two cauline leaves were collected from 5- and 6-wk-old plants and arranged on a black fabric in the order of leaf number. Bars, 5 cm. (b) RNA expression levels of senescence-related genes (*BFN1*, *NYE1*, *SAG29* and *VNI2*) were analyzed by qRT-PCR in leaves of 2-, 5- and 6-wk-old WT and *ubp12-2w/13-3* plants. Gene expression levels were normalized to that of leaves collected from 2-wk-old WT, which was set as 1. All rosette leaves were used for qRT-PCR experiments. All qRT-PCR experiments were performed in triplicate. Average results of three independent biological experiments ($n = 3$) are shown (±SD). *ACT2* expression levels were used as a control for normalization. *, $P < 0.05$; **, $P < 0.01$ (two-tailed *t*-test). (c) Total Chl content in WT and *ubp12-2w/13-3* were measured in all rosette leaves from 2-, 5- and 6-wk-old plants under normal growth conditions ($n = 6$ independent biological experiments). *, $P < 0.05$; **, $P < 0.01$ (two-tailed *t*-test); Ca, Chl*a*; Cb, Chl*b*. (d) Delayed leaf senescence of *ubp12-2w/13-3* under nitrogen-deficient conditions. Three-week-old seedlings of WT and *ubp12-2w/13-3* were transferred onto nitrogen containing (+N) or nitrogen deficient (−N) solid medium and grown for an additional 3 wk. All rosette leaves including petioles were excised and arranged on a black fabric in the order of leaf number. Leaves were distributed into four groups (marked 1–4) with group 1 containing leaf number 1 and 2, etc. Bar, 5 mm. (e) Total Chl content in leaves of WT and *ubp12-2w/13-3* plants grown under nitrogen-deficient conditions ($n = 6$). Leaves of groups 1–4 as shown in (d) were used. *, $P < 0.05$; **, $P < 0.01$ (two-tailed *t*-test); Ca, Chl*a*; Cb, Chl*b*. (f) Changes in RNA expression levels of *BFN1*, *SAG29*, *NYE1* and *ORE1* during nitrogen starvation. Two-week-old WT and *ubp12-2w/13-3* seedlings were transferred to nitrogen-deficient medium (−N) and samples were taken at the indicated time for qRT-PCR analysis. Expression value in 0 d of WT was set as 1. All qRT-PCR experiments were performed in three technical replicates and normalized with *ACT2*. Average values of three independent biological samples ($n = 3$) were presented (±SD).

© 2019 The Authors
New Phytologist © 2019 New Phytologist Trust

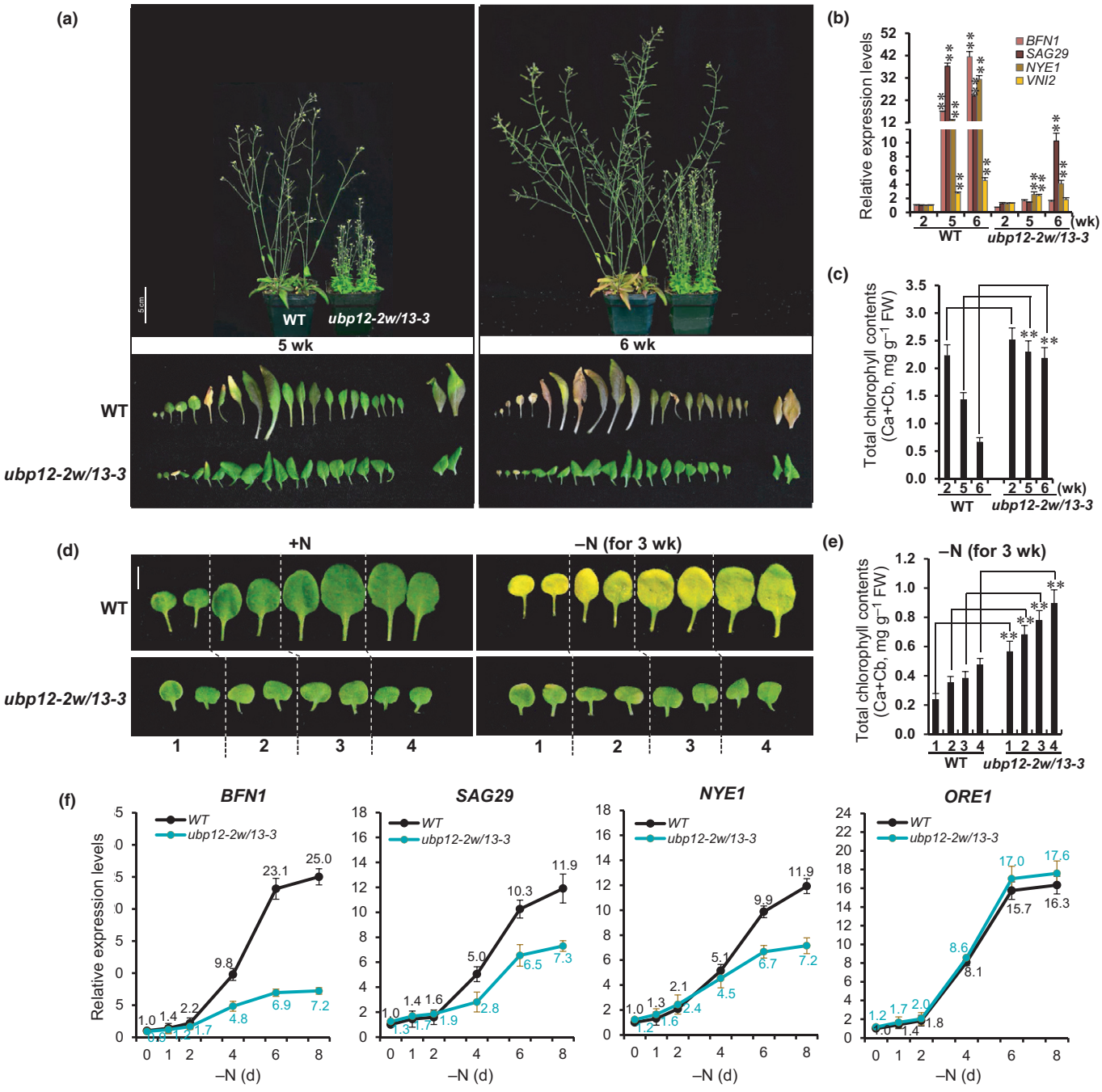

that UBP12/UBP13 function as positive regulators of age-dependent senescence.

In addition to the delayed age-dependent senescence, *ubp12-2w/13-3* plants displayed several morphological phenotypes which were not investigated in detail here (Figs 1a,d, S1). Seedlings of double mutant plants had shorter primary roots. Mature double mutant plants were smaller in stature but flowered early, and vegetative and floral organs were smaller as compared to WT plants.

To study the effects of nitrogen deficiency on leaf senescence, we investigated the leaf senescence phenotype of WT and *ubp12-2w/13-3* plants under nitrogen-sufficient or -deficient conditions. Three-week-old seedlings of WT and *ubp12-2w/13-3* plants were transferred and grown under nitrogen sufficient (+N) or nitrogen deficient (−N) conditions for an additional 3 wk. All leaves of WT turned yellow whereas only a slight change in color was detected in leaves of *ubp12-2w/13-3* (Fig. 1d). We categorized leaves into four groups (marked with 1–4) with group 1 containing leaf number 1 and 2, and so on. Total Chl content of WT leaves was about 2- to 3-fold lower than that of *ubp12-2w/13-3* leaves under −N conditions (Fig. 1e). The oldest WT leaves contained the lowest amount of Chl.

© 2019 The Authors
New Phytologist © 2019 New Phytologist Trust

We compared changes in gene expression levels during the first 8 d of −N treatment. The NAC transcription factor ORE1 is the major positive regulator of leaf senescence in *Arabidopsis* plants (Kim *et al.*, 2009; Balazadeh *et al.*, 2010). In WT seedlings, *ORE1* transcript levels were induced at day 2 in −N medium and reached a plateau value between days 6 and 8. Expression levels of senescence-related genes (*BFN1*, *SAG29* and *NYE1*) followed similar kinetics, consistent with their being downstream genes of *ORE1* (Fig. 1f). Plants of the *ubp12-2w/13-3* double mutant showed similar kinetics of induction for *ORE1* transcripts. By contrast, transcript levels of the three senescence-related genes reached only 30–60% of the WT values at day 8. *UBP12* and *UBP13* RNA expression in WT seedlings were also increased by nitrogen starvation (Fig. S2). The similar *ORE1* transcript levels in WT and *ubp12-2w/13-3* but reduced expression of the three downstream target genes in the double mutant compared to WT suggest possible reduced ORE1 protein levels in the double mutant.

UBP12/UBP13 interact with ORE1 *in vitro*

Park *et al.* (2018) have recently reported that ORE1 is unstable in WT plants subjected to nitrogen starvation. The instability of ORE1 is due to its ubiquitination by the NLA E3 ligase and subsequent destruction by 26S proteasomes. We hypothesized that UBP12/UBP13 execute their positive regulatory effect on leaf senescence via ORE1. To explore this hypothesis, we first tested whether UBP12 and UBP13 would interact with ORE1 *in vitro*. Fig. 2 shows that GST-UBP12 and GST-UBP13 were indeed able to bind to MBP-ORE1-myc *in vitro*. Under the same conditions, MBP-ORE1-myc did not bind to GST or GST-UBP14, both of which served as negative controls (Fig. 2). Additional binding specificity was shown by the lack of association between UBP12/UBP13 and MBP-NAC1-myc, another NAC domain protein.

UBP12/UBP13 interact with ORE1 *in vivo*

The *in vitro* interaction between UBP12/UBP13 and ORE1 suggested that they may also associate *in vivo*. We performed three different experiments to test this possibility. First, we used *N. benthamiana* leaves to transiently express *35S:ORE1-HA/UBQ10:UBP12-myc* and *35S:ORE1-HA/UBQ10:UBP13-myc* and prepared leaf extract for Co-IP. Fig. 3a) shows that ORE1-HA was present in the immunoprecipitates of UBP12-myc and UBP13-myc, indicating their association *in vivo*. Negative control experiments showed that UBP12/UBP13 did not interact with NAC1 and that ORE1 did not associate with UBP14. Second, these results were confirmed by Co-IP using *Arabidopsis* transgenic plants harboring either *XVE:UBP12-myc/35S:ORE1-HA* or *XVE:UBP13-myc/35S:ORE1-HA*. MG132 was added to inhibit 26S proteasome-mediated protein degradation. Association of UBP12-myc and UBP13-myc with ORE1-HA was detected only in plants treated with the β-estradiol inducer (Fig. 3b). Finally, BiFC assays performed in tobacco leaves showed clearly nYFP-ORE1 interacted with UBP12-cYFP and/

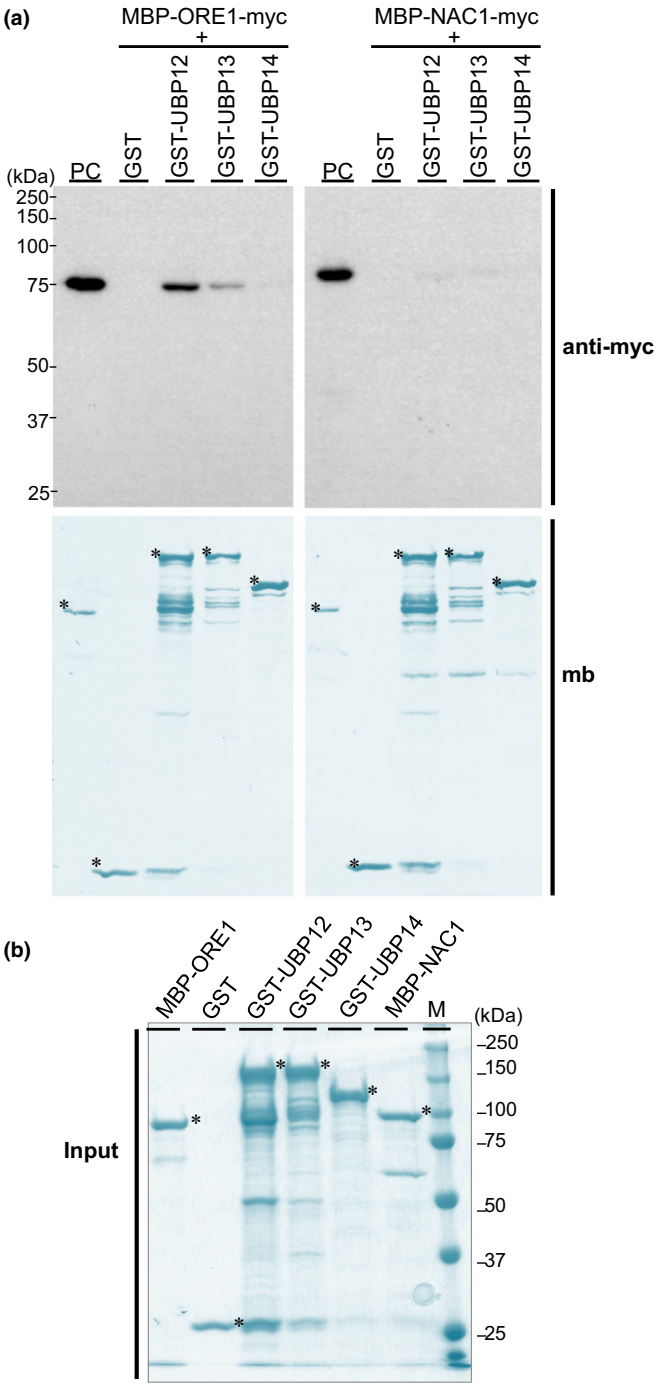

Fig. 2 UBP12/UBP13 and ORE1 interaction *in vitro*. (a) MBP-ORE1-myc and MBP-NAC1-myc were pulled down by GST, GST-UBP12, GST-UBP13 and GST-UBP14. NAC1 and UBP14 were used as negative controls. Positive control (PC) lanes for MBP-ORE1-myc and MBP-NAC1-myc contained 50 ng of proteins. Bands were detected by immunoblots using anti-myc. Membranes (mb) were stained with Coomassie Brilliant Blue. Asterisks (*) indicate the expected position of the recombinant protein. (b) Coomassie Brilliant Blue-stained SDS-PAGE gel of input proteins. Two micrograms of each protein was used in all experiments. The BSA band was used as a positive control. Asterisks (*) indicate the expected position of the recombinant protein. MBP, maltose binding protein; GST, glutathione-*S*-transferase; M, protein markers; kDa, kilodaltons.

© 2019 The Authors
New Phytologist © 2019 New Phytologist Trust

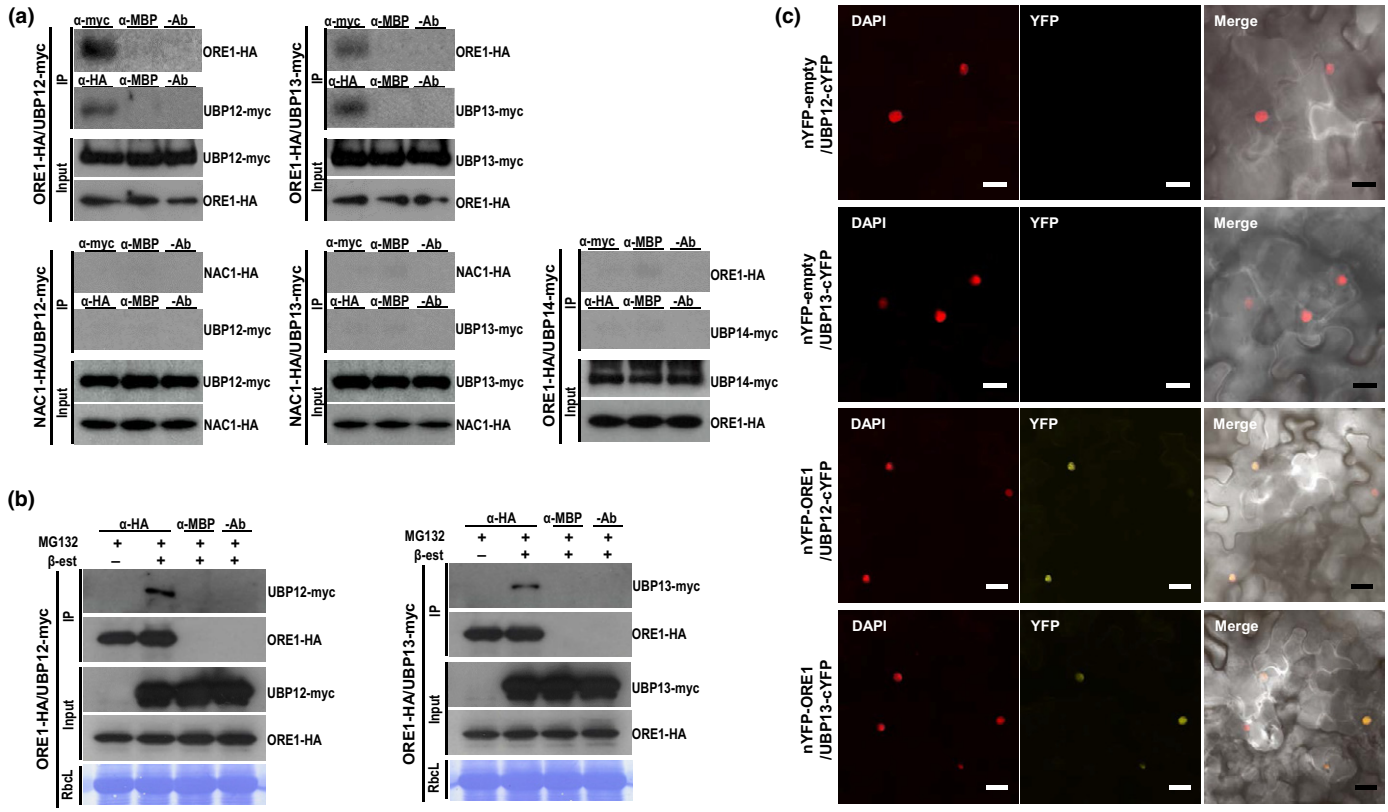

Fig. 3 UBP12 and UBP13 interact with ORE1 *in vivo*. (a) Interaction of UBP12/UBP13 and ORE1 in tobacco (*Nicotiana benthamiana*) leaves. Different combinations of *Agrobacterium* cultures were mixed and co-infiltrated into tobacco leaves for 3 d: the combinations were *35S:ORE1-HA/UBQ10:UBP12-myc*, *35S:ORE1-HA/UBQ10:UBP13-myc*, *35S:NAC1-HA/UBQ10:UBP12-myc*, *35S:NAC1-HA/UBQ10:UBP13-myc* and *35S:ORE1-HA/35S:UBP14-myc*. UBP12-myc, UBP13-myc and UBP14-myc proteins were immunoprecipitated with antibody α-myc and α-MBP or without antibody (-Ab) and ORE1-HA and NAC1-HA proteins in the immunoprecipitates detected by immunoblotting using α-HA antibody. In separate experiments, ORE1-HA and NAC1-HA proteins were immunoprecipitated with antibody α-HA and α-MBP or -Ab, and subsequently UBP12-myc, UBP13-myc and UBP14-myc proteins were detected by immunoblotting using α-myc antibody. Input proteins are shown. (b) *In vivo* interaction of UBP12/UBP13 and ORE1 in transgenic *Arabidopsis thaliana* (Col-0) plants expressing *XVE:UBP12-myc/35S:ORE1-HA* and *XVE:UBP13-myc/35S:ORE1-HA*. Ten-day-old seedlings were treated with 50 μM MG132 and 25 μM β-estradiol (β-est) for 16 h. UBP12-myc and UBP13-myc proteins were induced by β-est. ORE1 protein was immunoprecipitated with antibody α-HA and α-MBP or without antibody (-Ab) and UBP12-myc and UBP13-myc in the immunoprecipitates were analyzed by immunoblotting assay using α-myc antibody. Input proteins are shown. RbcL (the large subunit of RUBISCO) levels were used as loading controls. (c) Bimolecular fluorescence (BiFC) analysis of the interaction between UBP12/UBP13 and ORE1 in tobacco (*N. benthamiana*) leaves. Reconstituted yellow fluorescent protein (YFP) signals were detected in the nucleus of tobacco leaf cells when nYFP-ORE1 was transiently co-expressed with UBP12-cYFP or UBP13-cYFP in leaves infiltrated with *Agrobacterium*. Localization is shown by merging DAPI, YFP and DIC images (Merge). Confocal microscopic images were taken 2 d after infiltration. DAPI, 4′,6-diamidino-2-phenylindole; DIC, differential interference contrast. Bars, 20 μm.

or UBP13-cYFP in the nucleus (Fig. 3c). Collectively, these results provide evidence that UBP12 and UBP13 associate with ORE1 *in vitro* and *in vivo*.

UBP12 and UBP13 deubiquitinate polyubiquitinated ORE1 *in vitro*

To test for ORE1 deubiquitination *in vitro*, ORE1 was first polyubiquitinated by NLA (Park *et al.*, 2018). The polyubiquitinated ORE1 was then used as a substrate to test for possible deubiquitinating activity of UBP12 and UBP13 (Jeong *et al.*, 2017). Both short- and long-term time course experiments were performed (Fig. 4a,b). The amount of polyubiquitinated ORE1 was reduced 1 or 2 h after adding UBP12 or UBP13, whereas no change was detected with UBP14, which was used as a negative control. By contrast, the deubiquitination activity of UBP13 was lower than that of UBP12 (Fig. 4a). The amount of polyubiquitinated ORE1 was reduced 4 h after adding UBP12 and the polyubiquitinated bands disappeared at 8 h, compared with UBP14 (Fig. 4b). Because UBP12/UBP13 also is associated with NLA (Fig. S3), we investigated their activities using polyubiquitinated NLA. Fig. 4(c) shows that these two UBPs were inactive toward NLA. Our results show that the two UBPs possess deubiquitination activity for ORE1 but not for NLA.

UBP12 and UBP13 lead to leaf senescence by regulating ORE1 under N deficiency

Our finding that UBP12 and UBP13 can deubiquitinate polyubiquitinated ORE1 *in vitro* suggested that these two UBPs may

© 2019 The Authors
New Phytologist © 2019 New Phytologist Trust

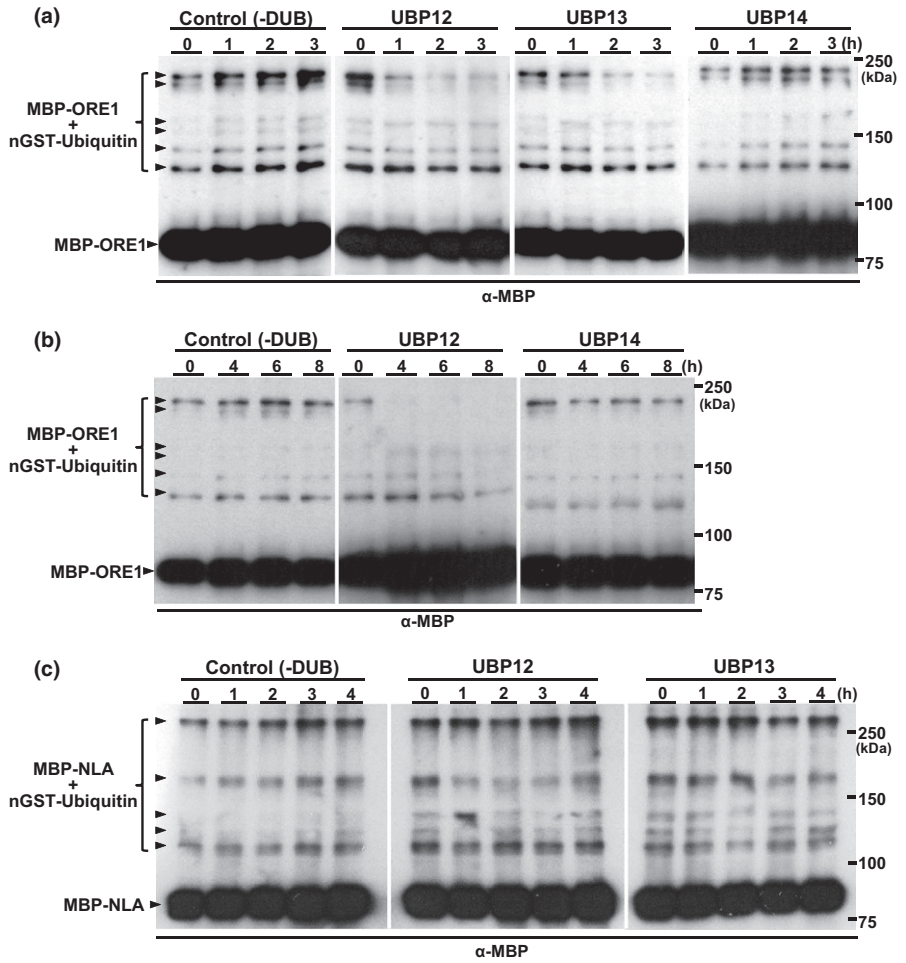

Fig. 4 UBP12/UBP13 deubiquitinate polyubiquitinated ORE1. Polyubiquitinated MBP-ORE1 proteins were prepared by incubating MBP-ORE1 with enzyme E1 (UBE1, yeast), E2 (UbcH6, human), E3 (GST-NLA) and ubiquitin fused with GST (nGST-Ubiquitin, 35 kDa). Auto-polyubiquitinated MBP-NLA was obtained by mixing MBP-NLA with E1, E2 and nGST-ubiquitin. Control (−DUB) sample contained distilled H_2O instead of DUB enzyme. Arrowheads indicate mono-, di-, tri-, tetra-, penta-, hexa- and hepta-ubiquitinated proteins from bottom to top. All bands were detected by immunoblotting assay using α-MBP antibody. MBP, maltose binding protein; GST, glutathione-*S*-transferase; kDa, kilodaltons. (a) Short-term time course (1–3 h) of deubiquitination of polyubiquitinated MBP-ORE1. Polyubiquitinated MBP-ORE1 was treated with 500 ng GST-UBP12, GST-UBP13 and GST-UBP14 for 1, 2 and 3 h. UBP14 was used as a negative control. (b) Long-term time course (4–8 h) of deubiquitination of polyubiquitinated MBP-ORE1. Polyubiquitinated MBP-ORE1 was treated with 500 ng GST-UBP12 and GST-UBP14 for 4, 6 and 8 h. UBP14 was used as a negative control. (c) UBP12 and UBP13 do not deubiquitinate polyubiquitinated NLA. GST-UBP12 and GST-UBP13 enzymes were mixed with polyubiquitinated MBP-NLA for 1, 2, 3 and 4 h.

promote senescence by maintaining ORE1 levels *in vivo*. To investigate this hypothesis, we explored the genetic interaction between *UBP12*/*UBP13* and *ORE1*. We constructed all possible double and triple mutants by genetic crosses and generated plants overexpressing *ORE1*, *UBP12* and *UBP13* in WT and various mutant backgrounds, and also double overexpression plants. Seedlings of these various genotypes were grown on nitrogen deficient (−N) medium for 2 wk to investigate senescence phenotype, total Chl content and senescence-related gene expression. We selected an −N treatment for 2 wk because seedlings that were grown on −N conditions for 3 wk showed leaf chlorosis (Fig. S4).

After 2 wk of N starvation leaves 1–4 of WT seedlings turned yellow and showed clear signs of senescence whereas the younger leaves (leaves 5–8) stayed green (Fig. 5a). Senescence of WT leaves 1–4 was completely or partially blocked in *ore1*, *ubp12-2w*, *ubp13-3*, *ubp12-2w/13-3* and *ubp12-2w/13-3/ore1*. By contrast, all eight leaves of *nla* seedlings turned yellow rapidly as reported (Park *et al.*, 2018). We also checked seedlings overexpressing *ORE1*, *UBP12* or *UBP13*. Leaves of $ORE1^{OE}$, $UBP12^{OE}$ and $UBP13^{OE}$ turned yellow or yellowish green faster than WT (Fig. 5a left panel) and after 2 wk of N starvation leaves 1–4 of overexpressing plants were clearly yellow, whereas WT leaves 1–4 were yellowish green under the same conditions. Taken together, these results support the view that UBP12 and UBP13 are positive regulators of senescence. To establish the relationship between UBP12/UBP13 and ORE1, we analyzed the phenotype of $UBP12^{OE}$/*ore1* and $UBP13^{OE}$/*ore1* plants. The senescence-promoting capacity of UBP12/UBP13 was totally

© 2019 The Authors
New Phytologist © 2019 New Phytologist Trust

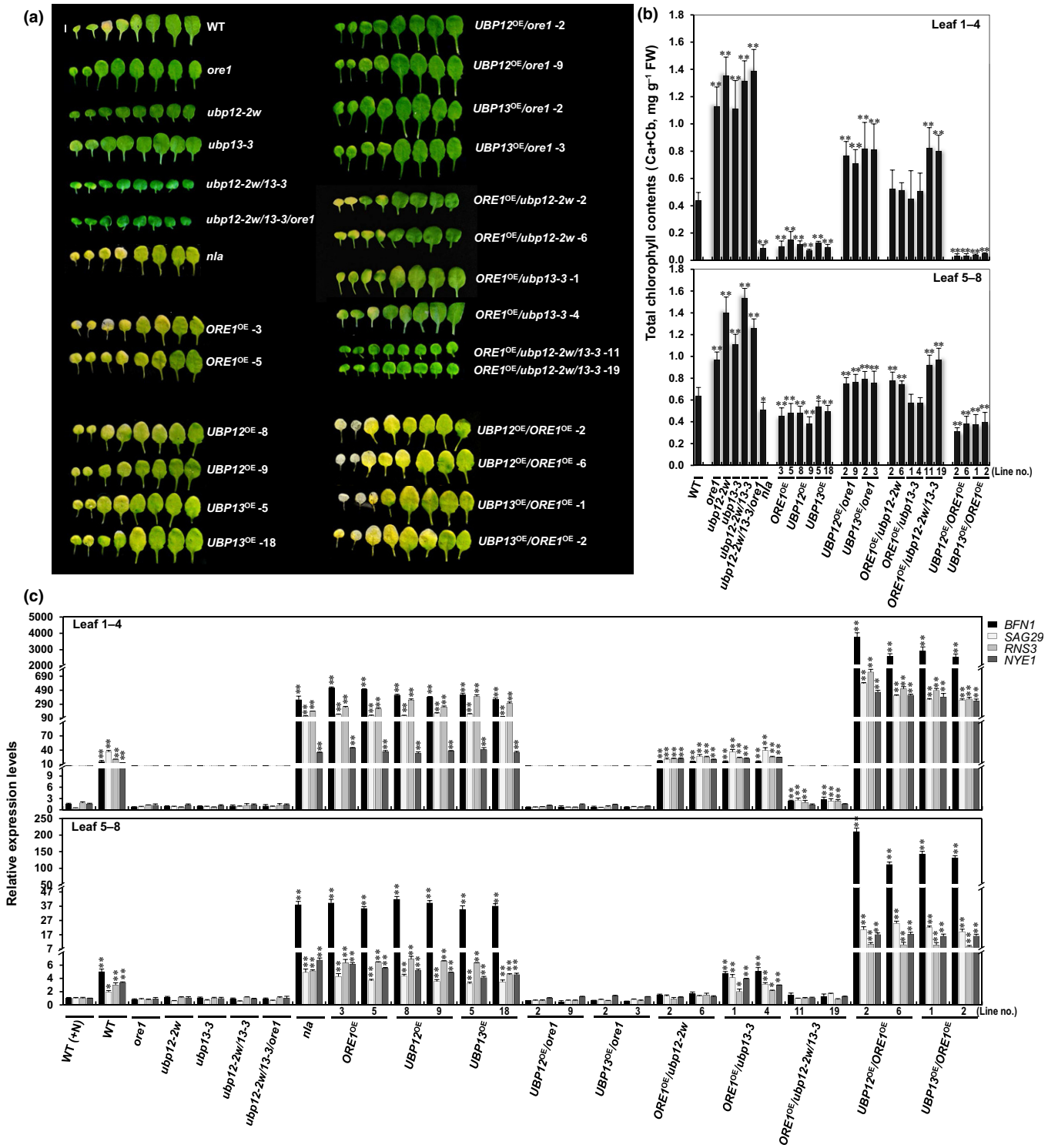

Fig. 5 Leaf senescence phenotype in *Arabidopsis thaliana* (Col-0) plants of various genotypes under nitrogen-deficient conditions. Three-week-old seedlings of various genotypes were transferred onto nitrogen-deficient (−N) solid medium and grown for an additional 2 wk. (a) Comparison of leaf senescence between various genotypes under −N conditions. After growth on −N solid medium for 2 wk, excised rosette leaves were arranged on a black fabric in the order of leaf number. Two different lines of each transgenic genotype were analyzed and shown. Six independent biological experiments were performed and images from one representative experiment are shown. Bar (top left corner), 5 mm. (b) Total leaf Chl content of all genotypes after growth under −N conditions. Leaves were divided into two groups: leaves 1–4 and 5–8. Average values of six independent biological experiments are shown (±SD) compared to WT ($n = 6$). *, $P < 0.05$; **, $P < 0.01$ (two-tailed *t*-test). (c) RNA expression levels of *BFN1*, *SAG29*, *RNS3* and *NYE1* analyzed by qRT-PCR in the two leaf groups (leaf numbers 1–4 and 5–8) from plants grown under −N conditions. Expression levels of WT (leaves 5–8) under nitrogen-sufficient conditions (+N) were set as 1. All qRT-PCR experiments were performed in triplicate. Average values of three independent biological samples ($n = 3$) are presented (±SD) compared to WT (+N) using two-tailed *t*-test (*, $P < 0.05$; **, $P < 0.01$). *ACT2* expression levels were used as a control for normalization.

© 2019 The Authors
New Phytologist © 2019 New Phytologist Trust

blocked by the *ore1* mutation, suggesting that ORE1 functions downstream of UBP12/UBP13. By contrast, the overexpression phenotype of *ORE1* (*ORE1*^{OE}) reverted to that of WT seedlings by *ubp12-2w* and *ubp13-3*, and in the case of *ubp12-2w/13-3,* the plants displayed delayed senescence. In *UBP12*/*ORE1* and *UBP13*/*ORE1* double overexpression plants the senescence phenotype was exacerbated compared to *nla* and *ORE1*^{OE} plants (Fig. 5a).

The senescence phenotype scored visually was corroborated by measurement of total Chl content. Fig. 5b) shows that leaf Chl content closely paralleled the visual phenotype in all plants examined. Moreover, leaf Chl content was inversely related to transcript levels of senescence-related genes, as was found in the experiments described in Fig. 1 (Fig. 5c). Taken together, these results suggest that UBP12 and UBP13 function as positive regulators of ORE1 to accelerate leaf senescence under N starvation.

UBP12 and UBP13 stabilize ORE1 protein

Thus far, we have shown that the ability of the UBPs to promote senescence depends on the presence of ORE1, an important transcriptional regulator of senescence-related genes. By contrast, the attenuation of the ORE1 overexpression phenotype by UBP12/UBP13 deficiencies suggests that UBP12 and UBP13 are required to maintain full activity of ORE1 *in vivo*. Because we have shown that UBP12/UBP13 can remove ubiquitin from polyubiquitinated ORE1 *in vitro*, we hypothesized that these UBPs have the same function *in vivo*, thereby rescuing ORE1 from destruction by 26S proteasomes. If this hypothesis is valid, we would expect ORE1 to be unstable and its protein levels to be increased by overexpression of UBP12/UBP13. However, ORE1 would be even more unstable in the *ubp12-2w/13-3* double mutant background.

To see if changes in UBP12 and UBP13 levels affected ORE1 protein stability, we compared ORE1-HA protein levels among four genotypes: *ORE1*^{OE}, *UBP12*^{OE}/*ORE1*^{OE}, *UBP13*^{OE}/*ORE1*^{OE} and *ORE1*^{OE}/*ubp12-2w/13-3* (Fig. S5). For these experiments, we selected transgenic lines with similar *ORE1-HA* transcript levels. Ten-day-old seedlings were transferred to nitrogen-deficient (−N) liquid medium and incubated for an additional 4 d. Two different lines of each transgenic genotype as shown in Fig. 5 were treated with or without 50 μM MG132 and ORE1-HA protein levels were analyzed by immunoblotting (Fig. 6a). In the untreated *ORE1*^{OE} line, ORE1-HA proteins were detected as

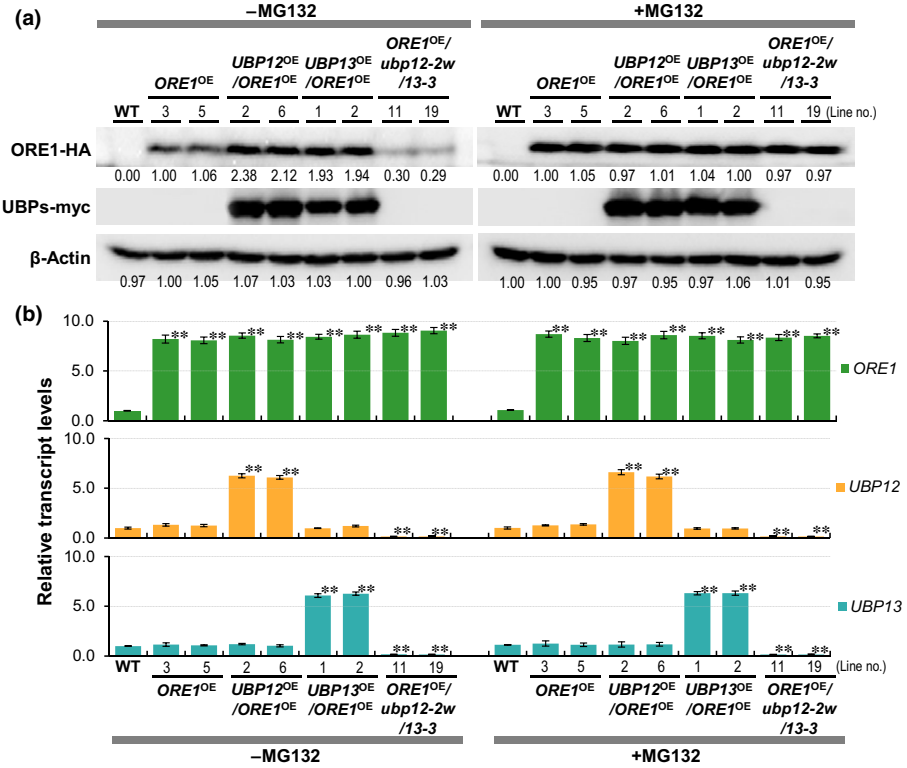

Fig. 6 UBP12 and UBP13 stabilize ORE1 protein *in vivo*. Ten-day-old *Arabidopsis thaliana* (Col-0) seedlings of *ORE1*^{OE}, *UBP12*^{OE}/*ORE1*^{OE}, *UBP13*^{OE}/*ORE1*^{OE} and *ORE1*^{OE}/*ubp12-2w/13-3* were transferred to nitrogen-deficient liquid medium and incubated for an additional 4 d. Two different lines of each transgenic genotype as marked in Fig. 5 were treated with or without 50 μM MG132 for 16 h ($n = 3$ biological replicates). (a) UBP12 and UBP13 stabilize ORE1 protein *in vivo*. ORE1-HA proteins from Mock (−MG132) and MG132-treated (+MG132) plants were analyzed by immunoblotting with anti-HA antibody. UBP12-myc and UBP13-myc proteins were only detected by anti-myc antibody in *UBP12*^{OE}/*ORE1*^{OE} and *UBP13*^{OE}/*ORE1*^{OE} plants. Expression levels of *ORE1*^{OE} in line no. 3 were set as 1. WT was used as a negative control. β-Actin levels were used as a loading control. (b) Quantitative RT-PCR analysis of *ORE1*, *UBP12* and *UBP13* transcript levels of four genotypes under treatment with/without 50 μM MG132. Whole seedlings were used for immunoblotting and qRT-PCR analysis. Expression levels of three transcripts were examined by qRT-PCR with primers specific for each coding sequence. All qRT-PCR experiments were performed in triplicate. Expression values of WT were set as 1. Average values from three independent biological experiments ($n = 3$) are shown (±SD). *ACT2* expression levels were used as a control for normalization. *, $P < 0.05$; **, $P < 0.01$ (two-tailed *t*-test).

© 2019 The Authors
New Phytologist © 2019 New Phytologist Trust

a faint band whose intensity was considerably increased by MG132, which arrests protein degradation. No change in *ORE1* transcript levels was detected with addition of MG132 (Fig. 6b). These results indicate that ORE1 protein is very unstable under normal conditions. The low ORE1 levels in untreated samples can be increased by the expression of $UBP12^{OE}$ or $UBP13^{OE}$ and the addition of MG132 had only a modest effect, indicating that these UBPs are able to mimic MG132 to block ORE1 protein degradation shown in the WT background. In $ORE1^{OE}$/*ubp12-2w/13-3* plants, ORE1-HA protein levels were even lower than those in $ORE1^{OE}$ plants with comparable *ORE1* transcript levels but ORE1-HA levels were the same as those of $ORE1^{OE}$/WT plants after MG132 treatment. In all cases, *ORE1* transcript levels of all genotypes were not affected by MG132 treatment (Fig. 6b).

We determined the half-life of ORE1-HA under different levels of *UBP12* and *UBP13* expression to investigate whether ORE1-HA is directly affected by levels of UBP12 and UBP13. Cycloheximide (CHX)-chase experiments were conducted in four genotypes: $ORE1^{OE}$, $UBP12^{OE}$/$ORE1^{OE}$, $UBP13^{OE}$/$ORE1^{OE}$ and $ORE1^{OE}$/*ubp12-2w/13-3* (Fig. 7). In these experiments, plants were first treated with MG132 for 16 h to accumulate ORE1-HA protein. MG132 was then removed by repeated washings and the seedlings were transferred to a medium containing CHX which blocks new protein synthesis. Seedlings were then harvested at different times to determine ORE1-HA protein levels. In $ORE1^{OE}$ plants, the half-life of the ORE1-HA protein was around 50 min. The protein half-life was reduced to about 18 min in $ORE1^{OE}$/*ubp12-2w/13-3* plants. By contrast, overexpression of *UBP12* and *UBP13* prolonged the half-life of ORE1-HA to > 100 min. These results show that UBP12 and UBP13 directly function as positive regulators of ORE1 by increasing the stability of ORE1 protein *in vivo*.

Discussion

Loss-of-function mutants deficient in UBP12/UBP13 display a variety of morphological phenotypes, suggesting that these two ubiquitin proteases with redundant functions probably play important roles in plant growth and development. It is clear that further understanding of the molecular basis of UBP12/UBP13 function would require identification of their substrates. So far, UBP12/UBP13 have been reported to deubiquitinate H2Aub (Derkacheva *et al.*, 2016) and MYC2 (Jeong *et al.*, 2017), and also to bind to RGF1 (An *et al.*, 2018). Here, we have provided several lines of evidence supporting our claim that the NAC-domain transcription factor ORE1, which is a key positive regulator of leaf senescence, is also a target of UBP12/UBP13: that is, UBP12/UBP13 bind to ORE1 *in vitro* and *in vivo*; UBP12/UBP13 have the capacity to deubiquitinate polyubiquitinated ORE1 *in vitro*, suggesting that they may execute similar function *in vivo*; expression of UBP12/UBP13 increases ORE1 protein levels without changing *ORE1* transcript levels; and consistent with the observed effects of UBP12/UBP13 on ORE1 levels nitrogen-deficiency-induced leaf senescence of *ubp12-2w/13-3* is delayed compared to WT whereas overexpression of UBP12/UBP13 causes accelerated senescence.

UBP12 and UBP13 counteract the effects of NLA

As the key transcription factor regulating senescence, ORE1 activates several downstream senescence-related genes. Therefore, it is not surprising that ORE1 levels are fine-tuned by both positive and negative factors allowing plants to sense and respond rapidly to the changing environment. We have recently shown that the ORE1 protein is unstable owing to ubiquitin-mediated degradation and we have identified its cognate E2 conjugase and E3

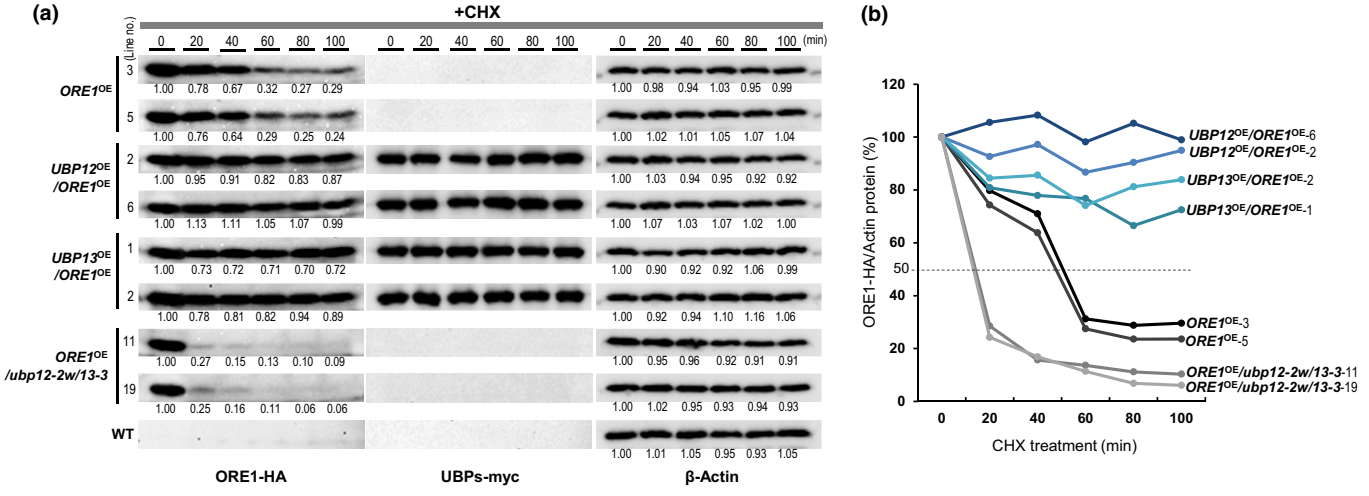

Fig. 7 UBP12 and UBP13 increase ORE1 stability. Ten-day-old *Arabidopsis thaliana* (Col-0) seedlings of $ORE1^{OE}$, $UBP12^{OE}$/$ORE1^{OE}$, $UBP13^{OE}$/$ORE1^{OE}$ and $ORE1^{OE}$/*ubp12-2w/13-3* were transferred to nitrogen-deficient liquid medium and incubated for an additional 4 d. Seedlings incubated with 50 μM MG132 for 16 h were washed and transferred to medium containing 200 μM cycloheximide. Two different lines of each transgenic genotype as marked in Fig. 5 were used as biological replicates. ORE1 protein levels were determined at 20, 40, 60, 80 and 100 min. (a) ORE1-HA, UBP12-myc and UBP13-myc proteins were detected by immunoblots using antibody anti-HA and anti-myc. β-Actin levels were used as loading controls. Band intensity of 0 time point was set as 1 and the values were measured by using ImageJ. (b) Changes in ORE1-HA levels. ORE1-HA protein levels were normalized with β-actin levels of each time point.

© 2019 The Authors
New Phytologist © 2019 New Phytologist Trust

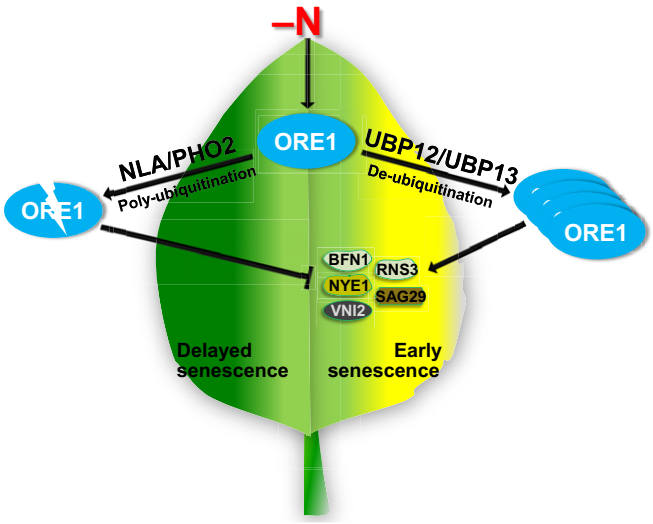

Fig. 8 UBP12 and UBP13 regulate ORE1 during leaf senescence under nitrogen-deficient (−N) conditions. ORE1 interacts with NLA and UBP12/UBP13. ORE1 is first polyubiquitinated by the E3/E2 enzyme complex, NLA/PHO2, and then degraded by 26S proteasomes leading to delayed leaf senescence (Park *et al*., 2018). When plants are exposed to nitrogen-deficient conditions (−N) UBP12 and UBP13 antagonize the effects of NLA E3 ligase by promoting the deubiquitination of polyubiquitinated-ORE1 and rescue ORE1 from being degraded. The elevated ORE1 levels activate expression of downstream genes such as *BFN1*, *RNS3*, *NYE1*, *VNI2* and *SAG29*, resulting in accelerated leaf senescence.

ligase as PHO2 and NLA, respectively (Park *et al*., 2018). The rapid degradation of ORE1 allows a faster recovery of nitrogen-stressed plants when nitrogen becomes available in the environment (Fig. 8). By contrast, similar to the case of phosphorylation and dephosphorylation, proteins decorated with polyubiquitin can be rescued from destruction by the action of deubiquitinating enzymes. Here, we provide evidence that UBP12 and UBP13 are probably the cognate ubiquitin proteases for ORE1 *in vivo*. Although the two UBPs have redundant function based on the overexpression phenotypes, it appears that UBP12 may be more active than UBP13. These two UBPs oppose the function of NLA so that the onset of senescence can occur faster when plants are starved of nitrogen (Fig. 8). We found that although NLA associates with UBP12 and UBP13 *in vitro*, it is not deubiquitinated by the two UBPs (Figs S3, 4c). It would be interesting to investigate how environmental factors regulate the activities of positive and negative regulators in the NLA/UBP12 and/or NLA/UBP13 complex.

Multiple functions of UBP12 and UBP13

The *Arabidopsis* genome encodes only 64 potential DUBs (Isono & Nagel, 2014) compared with the > 1400 ubiquitin ligases (Vierstra, 2009; Wang & Deng, 2011). Therefore, it is very likely that each DUB manages multiple cellular targets. The ortholog of UBP12/UBP13 in humans is the ubiquitin-specific protease 7 (USP7 or Herpes-Associated Ubiquitin-Specific Protease, HAUSP) which targets several proteins including p53 and MDM2 to promote apoptosis, histone H2Bub to repress a set of genes and RING1B of the PRC1 complex to prevent its RING domain from being self-ubiquitinated (Cummins & Vogelstein, 2004; Brazhnik & Kohn, 2007; McClurg & Robson, 2015; Lecona *et al*., 2016; Kim & Sixma, 2017).

Although the role of UBP12 and UBP13 was characterized first in plant immunity including SA response (Ewan *et al*., 2011) and then subsequently in circadian clock and plant development (Cui *et al*., 2013) the mechanisms of action of UBP12/UBP13 in these processes remain largely unexplored. Recently, direct targets of UBP12 and UBP13 in several pathways have been described. These two UBPs function in epigenetic regulation of polycomb group protein by directly deubiquitinating histone H2A (Derkacheva *et al*., 2016), in the JA response through controlling the stability of a key regulator, MYC2 (Jeong *et al*., 2017), and in root meristem maintenance by regulating the stability of RGF1 (An *et al*., 2018).

Similar to their human homolog USP7, we consider that UBP12 and UBP13 are likely to regulate several additional cellular targets waiting identification. As shown in Fig. S1, under normal conditions, the *ubp12-2w/13-3* mutant shows various phenotypes in leaf size, hypocotyl length, root length, flower size, silique size and seed size. Here, we have only investigated the function of UBP12/UBP13 under nitrogen deficiency. It would be important to extend similar studies to other stresses, such as dehydration, salinity and ABA. Moreover, the characterization of additional cellular targets of UBP12/UBP13 that function under specific environmental condition would probably advance our understanding of the mechanism regulating these developmental processes.

When nutrients become limiting, plants begin to disassemble chloroplasts through senescence so as to recycle stored nutrients and remobilize them to growing tissues (Have *et al*., 2017). It has been estimated that up to 80% of nitrogen is remobilized during leaf senescence (Himelblau & Amasino, 2001). Natural leaf senescence is an essential process for normal seed development and seed set. By contrast, rapid leaf senescence triggered by certain stresses leads to immature seed or even seed abortion. Despite its early flowering, the *ubp12-2w/13-3* double mutant has strongly reduced seed set compared to WT due to delayed leaf senescence (Fig. S1). On the other hand, flowering time and seed set appear unchanged in plants overexpressing *ORE1*, *UBP12* and *UBP13* compared to WT under normal growth conditions. However, we suggest that seed set of these overexpressing plants might be increased compared to WT due to accelerated leaf senescence under nitrogen deficiency.

Most transcription factors are unstable so that they can respond to rapid changes in signals sometimes working in opposition. Previous work shows that the instability of ORE1 is largely due to NLA, its cognate E3 ligase (Park *et al*., 2018), and here we show that UBP12/UBP13 can counteract the effects of NLA to stabilize the transcription factor. Such fine-tuning of ORE1 levels gives plants the flexibility to adjust rapidly to the fluctuating nitrogen levels in the environment. The identification of key regulators of ORE1 reported before (Park *et al*., 2018) and also described here suggest important strategies to generate crop

© 2019 The Authors
New Phytologist © 2019 New Phytologist Trust

plants with increased nitrogen use efficiency and with reduced senescence.

Acknowledgements

This work was supported in part by RSSS grant (no. NRF-RSSS-002) to N-HC from the National Research Foundation Singapore.

Author contributions

S-HP, JSJ, BSP and N-HC designed experiments, S-HP, JSJ and JSS performed experiments. S-HP and N-HC wrote the manuscript, which was reviewed by all.

ORCID

Nam-Hai Chua https://orcid.org/0000-0001-5931-3923
Jin Seo Jeong https://orcid.org/0000-0002-8926-7793
Bong Soo Park https://orcid.org/0000-0002-7726-2020
Su-Hyun Park https://orcid.org/0000-0002-9237-7600
Jun Sung Seo https://orcid.org/0000-0002-3420-8446

References

Agüera E, Cabello P, de la Haba P. 2010. Induction of leaf senescence by low nitrogen nutrition in sunflower (*Helianthus annuus*) plants. *Physiologia Plantarum* **138**: 256–267.

Amerik AY, Hochstrasser M. 2004. Mechanism and function of deubiquitinating enzymes. *Biochimica et Biophysica Acta* **1695**: 189–207.

An Z, Liu Y, Ou Y, Li J, Zhang B, Sun D, Sun Y, Tang W. 2018. Regulation of the stability of RGF1 receptor by the ubiquitin-specific proteases UBP12/UBP13 is critical for root meristem maintenance. *Proceedings of the National Academy of Sciences, USA* **115**: 1123–1128.

Arnon DI. 1949. Copper enzymes in isolated chloroplasts. Polyphenoloxidase in *Beta vulgaris*. *Plant Physiology* **24**: 1–15.

Balakirev MY, Tcherniuk SO, Jaquinod M, Chroboczek J. 2003. Otubains: a new family of cysteine proteases in the ubiquitin pathway. *EMBO Reports* **4**: 517–522.

Balazadeh S, Wu A, Mueller-Roeber B. 2010. Salt-triggered expression of the ANAC092-dependent senescence regulon in *Arabidopsis thaliana*. *Plant Signaling & Behavior* **5**: 733–735.

Brazhnik P, Kohn KW. 2007. HAUSP-regulated switch from auto- to p53 ubiquitination by Mdm2 (*in silico* discovery). *Mathematical Biosciences* **210**: 60–77.

Burnett B, Li F, Pittman RN. 2003. The polyglutamine neurodegenerative protein ataxin-3 binds polyubiquitylated proteins and has ubiquitin protease activity. *Human Molecular Genetics* **12**: 3195–3205.

Clough SJ, Bent AF. 1998. Floral dip: a simplified method for *Agrobacterium*-mediated transformation of *Arabidopsis thaliana*. *The Plant Journal* **16**: 735–743.

Cui X, Lu F, Li Y, Xue Y, Kang Y, Zhang S, Qiu Q, Cui X, Zheng S, Liu B *et al.* 2013. Ubiquitin-specific proteases UBP12 and UBP13 act in circadian clock and photoperiodic flowering regulation in Arabidopsis. *Plant Physiology* **162**: 897–906.

Cummins JM, Vogelstein B. 2004. HAUSP is required for p53 destabilization. *Cell Cycle* **3**: 689–692.

Derkacheva M, Liu S, Figueiredo DD, Gentry M, Mozgova I, Nanni P, Tang M, Annervik M, Köhler C, Hennig L. 2016. H2A deubiquitinases UBP12/13 are part of the Arabidopsis polycomb group protein system. *Nature Plants* **15**: 16126.

Diaz C, Lemaitre T, Christ A, Azzopardi M, Kato Y, Sato F, MorotGaudry JF, Le Dily F, Masclaux-Daubresse C. 2008. Nitrogen recycling and remobilization are differentially controlled by leaf senescence and development stage in Arabidopsis under low nitrogen nutrition. *Plant Physiology* **147**: 1437–1449.

Ewan R, Pangestuti R, Thornber S, Craig A, Carr C, O'Donnell L, Zhang C, Sadanandom A. 2011. Deubiquitinating enzymes AtUBP12 and AtUBP13 and their tobacco homologue NtUBP12 are negative regulators of plant immunity. *New Phytologist* **191**: 92–106.

Fujiwara T, Hirai MY, Chino M, Komeda Y, Naito S. 1992. Effects of sulfur nutrition on expression of the soybean seed storage protein genes in transgenic petunia. *Plant Physiology* **99**: 263–268.

Guo H-S, Xie Q, Fei J-F, Chua N-H. 2005. MicroRNA directs mRNA cleavage of the transcription factor NAC1 to downregulate auxin signals for Arabidopsis lateral root development. *Plant Cell* **17**: 1376–1386.

Have M, Marmagne A, Chardon F, Masclaux-Daubresse C. 2017. Nitrogen remobilization during leaf senescence: lessons from Arabidopsis to crops. *Journal of Experimental Botany* **68**: 2513–2529.

Himelblau E, Amasino RM. 2001. Nutrients mobilized from leaves of *Arabidopsis thaliana* during leaf senescence. *Journal of Plant Physiology* **158**: 1317–1323.

Hu M, Li P, Li M, Li W, Yao T, Wu JW, Gu W, Cohen RE, Shi Y. 2002. Crystal structure of a UBP-family deubiquitinating enzyme in isolation and in complex with ubiquitin aldehyde. *Cell* **111**: 1041–1054.

Isono E, Nagel M-K. 2014. Deubiquitylating enzymes and their emerging role in plant biology. *Frontiers in Plant Science* **5**: 56.

Jeong JS, Jung C, Seo JS, Kim J-K, Chua N-H. 2017. The deubiquitinating enzymes UBP12 and UBP13 positively regulate MYC2 levels in jasmonate responses. *Plant Cell* **29**: 1406–1424.

Jibran R, Hunter DA, Dijkwel PP. 2013. Hormonal regulation of leaf senescence through integration of developmental and stress signals. *Plant Molecular Biology* **82**: 547–561.

Johnston SC, Larsen CN, Cook WJ, Wilkinson KD, Hill CP. 1997. Crystal structure of a deubiquitinating enzyme (human UCH-L3) at 1.8 A resolution. *EMBO Journal* **16**: 3787–3796.

Johnston SC, Riddle SM, Cohen RE, Hill CP. 1999. Structural basis for the specificity of ubiquitin C-terminal hydrolases. *EMBO Journal* **18**: 3877–3887.

Khan M, Rozhon W, Poppenberger B. 2014. The role of hormones in the aging of plants. *Gerontology* **60**: 49–55.

Kim H, Kim HJ, Vub QT, Jung S, McClungc CR, Hong S, Nam HG. 2018. Circadian control of *ORE1* by PRR9 positively regulates leaf senescence in *Arabidopsis*. *Proceedings of the National Academy of Sciences, USA* **115**: 8448–8453.

Kim JH, Woo HR, Kim J, Lim PO, Lee IC, Choi SH, Hwang D, Nam HG. 2009. Trifurcate feed-forward regulation of age-dependent cell death involving miR164 in *Arabidopsis*. *Science* **323**: 1053–1057.

Kim RQ, Sixma TK. 2017. Regulation of USP7: a high incidence of E3 complexes. *Journal of Molecular Biology* **429**: 3395–3408.

Lecona E, Rodriguez-Acebes S, Specks J, Lopez-Contreras AJ, Ruppen I, Murga M, Munoz J, Mendez J, Fernandez-Capetillo O. 2016. USP7 is a SUMO deubiquitinase essential for DNA replication. *Nature Structural & Molecular Biology* **23**: 270–277.

Lim PO, Kim HJ, Nam HG. 2007. Leaf senescence. *Annual Review of Plant Biology* **58**: 115–136.

Liu Y, Wang F, Zhang H, He H, Ma L, Deng XW. 2008. Functional characterization of the Arabidopsis ubiquitin-specific protease gene family reveals specific role and redundancy of individual members in development. *The Plant Journal* **55**: 844–856.

Masclaux-Daubresse C, Daniel-Vedele F, Dechorgnat J, Chardon F, Gaufichon L, Suzuki A. 2010. Nitrogen uptake, assimilation and remobilisation in plants: challenges for sustainable and productive agriculture. *Annals of Botany* **105**: 1141–1158.

Matallana-Ramirez LP, Rauf M, Farage-Barhom S, Dortay H, Xue GP, Dröge-Laser W, Lers A, Balazadeh S, MuellerRoeber B. 2013. NAC transcription factor ORE1 and senescence-induced BIFUNCTIONAL NUCLEASE1 (BFN1) constitute a regulatory cascade in Arabidopsis. *Molecular Plant* **6**: 1438–1452.

© 2019 The Authors
New Phytologist © 2019 New Phytologist Trust

McClurg UL, Robson CN. 2015. Deubiquitinating enzymes as oncotargets. *Oncotarget* **6**: 9657–9668.

Meng S, Peng JS, He YN, Zhang GB, Yi HY, Fu YL, Gong JM. 2016. Arabidopsis NRT1.5 mediates the suppression of nitrate starvation-induced leaf senescence by modulating foliar potassium level. *Molecular Plant* **9**: 461–470.

Nanao MH, Tcherniuk SO, Chroboczek J, Dideberg O, Dessen A, Balakirev MY. 2004. Crystal structure of human otubain 2. *EMBO Reports* **5**: 783–788.

Nijman SM, Luna-Vargas MP, Velds A, Brummelkamp TR, Dirac AM, Sixma TK, Bernards R. 2005. A genomic and functional inventory of deubiquitinating enzymes. *Cell* **123**: 773–786.

Park BS, Seo JS, Chua N-H. 2014. NITROGEN LIMITATION ADAPTATION recruits PHOSPHATE2 to target the phosphate transporter PT2 for degradation during the regulation of Arabidopsis phosphate homeostasis. *Plant Cell* **26**: 454–464.

Park BS, Yao T, Seo JS, Chi E, Wong C, Mitsuda N, Huang C-H, Chua N-H. 2018. Arabidopsis NITROGEN LIMITATION ADAPTATION regulates ORE1 homeostasis during senescence induced by nitrogen deficiency. *Nature Plants* **4**: 898–903.

Qiu K, Li Z, Yang Z, Chen J, Wu S, Zhu X, Gao S, Gao J, Ren G, Kuai B *et al.* 2015. EIN3 and ORE1 accelerate degreening during ethylene-mediated leaf senescence by directly activating chlorophyll catabolic genes in Arabidopsis. *PLoS Genetics* **11**: e1005399.

Rauf M, Arif M, Dortay H, Matallana-Ramírez LP, Waters MT, Nam HG, Lim PO, Mueller-Roeber B, Balazadeh S. 2013. ORE1 balances leaf senescence against maintenance by antagonizing G2-like-mediated transcription. *EMBO Reports* **14**: 382–388.

Scheel H, Tomiuk S, Hofmann K. 2003. Elucidation of ataxin-3 and ataxin-7 function by integrative bioinformatics. *Human Molecular Genetics* **12**: 2845–2852.

Schulte auf'm Erley G, Begum N, Worku M, Bänzinger M, Horst WJ. 2007. Leaf senescence induced by nitrogen deficiency as an indicator of genotypic differences in nitrogen efficiency in tropical maize. *Journal of Plant Nutrition and Soil Science* **170**: 106–114.

Verma R, Aravind L, Oania R, McDonald WH, Yates JR, Koonin EV, Deshaies RJ. 2002. Role of Rpn11 metalloprotease in deubiquitination and degradation by the 26S proteasome. *Science* **298**: 611–615.

Vierstra RD. 2009. The ubiquitin-26S proteasome system at the nexus of plant biology. *Nature Reviews Molecular Cell Biology* **10**: 385–397.

Wang F, Deng XW. 2011. Plant ubiquitin-proteasome pathway and its role in gibberellin signaling. *Cell Research* **21**: 1286–1294.

Wilkinson KD. 1997. Regulation of ubiquitin-dependent processes by deubiquitinating enzymes. *FASEB Journal* **11**: 1245–1256.

Woo HR, Kim HJ, Nam HG, Lim PO. 2013. Plant leaf senescence and death-regulation by multiple layers of control and implications for aging in general. *Journal of Cell Science* **126**: 4823–4833.

Xie Q, Guo HS, Dallman G, Fang S, Weissman AM, Chua N-H. 2002. SINAT5 promotes ubiquitin-related degradation of NAC1 to attenuate auxin signals. *Nature* **419**: 167–170.

Yan N, Doelling JH, Falbel TG, Durski AM, Vierstra RD. 2000. The ubiquitin-specific protease family from Arabidopsis. AtUBP1 and 2 are required for the resistance to the amino acid analog canavanine. *Plant Physiology* **124**: 1828–1843.

Zhang X, Henriques R, Lin SS, Niu QW, Chua N-H. 2006. *Agrobacterium*-mediated transformation of *Arabidopsis thaliana* using the floral dip method. *Nature Protocols* **1**: 641–646.

Zhou H, Zhao J, Cai J, Patil SB. 2017. UBIQUITIN-SPECIFIC PROTEASES function in plant development and stress responses. *Plant Molecular Biology* **94**: 565–576.

Zuo J, Niu Q-W, Frugis G, Chua N-H. 2002. The WUSCHEL gene promotes vegetative-to-embryonic transition in Arabidopsis. *The Plant Journal* **30**: 349–359.

Supporting Information

Additional Supporting Information may be found online in the Supporting Information section at the end of the article.

Fig. S1 Developmental phenotypes in wild-type (WT) and *ubp12-2w/13-3* plants.

Fig. S2 Increase of *UBP12* and *UBP13* RNA expression during nitrogen starvation.

Fig. S3 UBP12 and UBP13 interact with NLA *in vitro* and *in vivo*.

Fig. S4 Leaf senescence phenotype in various genotypes under nitrogen sufficient and deficient conditions for 2 and 3 wk.

Fig. S5 Differences in ORE1 protein levels in plants expressing different levels of UBP12/UBP13 with and without MG132 treatment.

Table S1 Primers used in this study.

Please note: Wiley Blackwell are not responsible for the content or functionality of any Supporting Information supplied by the authors. Any queries (other than missing material) should be directed to the *New Phytologist* Central Office.

© 2019 The Authors
New Phytologist © 2019 New Phytologist Trust